A NEW INVENTORY OF MARTIAN LANDSLIDES

G.B. Crosta[(1)], P. Frattini[(1)], and E. Valbuzzi [(1)], [(1)] Università degli Studi di Milano-Bicocca, Dept. of Earth and Environmental Sciences (P.za della Scienza 4, 20126, Milano, Italy, giovannibattista.crosta@unimib.it)

Introduction: Martian landslides have been studied and mapped by different authors by using different approaches and tools [1], [2], [3], [4] and [5]. The available observations have also been used for modeling purposes and to understanding controlling mechanisms [6], [7] and [8].

Recently, large satellite imagery datasets have become available and they have been mosaicked in different suitable tools making mapping an easier job than before. Furthermore, the availability of other georeferenced database makes possible and easily feasible some spatially distributed analyses.

We prepared a new landslide inventory to acquire information about: landslide size distribution and areal density, controls of geometrical condition along Martian slopes, landslide typology and mechanism, relationship with impact craters distribution, runout, volume estimates, characteristic features.

The landslide inventory presently under completion includes about 1200 landslides and it covers a sector of Mars comprised between -37° N and 46° N latitude and 141° W and 142° E longitude.

This work is part of a larger effort aimed to a more quantitative description of landslide phenomena on Mars and the understanding of rock mass properties and landslide mobility with respect to their Earth equivalents (see also Abstract 1624 in this conference).

Methods: We adopted Google Mars® as a mapping tool using both visible images (global base map based on wide-angle imagery from Viking orbiters, MOC Mars Orbiter Camera, HRSC High-Resolution Stereo Camera, and HiRISE High-Resolution Imaging Science Experiment) and CTX images (MRO: Mars Reconnaissance Orbiter Context Camera - CTX- images).

Landslides have been map,ped according to standard geomorphological criteria, by two landslide experts delineating both the landslide scar and accumulation limits, associating each scarp to a deposit. Multiple accumulations have been differentiated where possible to obtain a more sound dataset.

We prevalently mapped landslides located along the Martian valleys and Chasma flanks with only minor attention to classical block and slump instabilities typical of crater rim failures. This because we were mainly interested in long runout landslides or complex failures which could allow to define some rock mass characteristics along these slopes, and to study landslide mobility with respect to Earth equivalent phenomena. So long runout landslides have been mapped also when recognized within crater rims.

Successively, the mapped elements have been transferred to ArcGIS (ESRI®) for spatial analyses. Topographic characteristics have been extracted by means of the available MOLA dataset.

Results: Presently, the database consists of 1232 landslides covering a total area of about 180,000 km^2. Landslide size ranges from 0.15 km^2 to a maximum of 12,000 km^2.

We examined area-frequency distributions of landslides by developing logarithmically binned, non-cumulative size frequency distributions that report frequency density (f = dN/dA) as a function of landslide planar area A (dN = number of landslides with an area between A and A+dA). The size frequency distribution presents a modal value of 0.8 km^2. For landslides larger than this value, the size frequency distribution exhibits a multifractal behaviour, that was interpolated with two power law functions:

$$f(A) = aA^{-b} \quad (1)$$

From 1 to 500 km^2 the scaling exponent, -b, equals to 1.11 (Fig. 2). For larger landslides, the scaling equals to -2.19. This last value is similar to those reported in the terrestrial landslide literature (e.g., 2.11-2.48, [9]).

Up to now total drop height ad maximum runout distance have been determined for about 500 landslides and these can be associated to the accumulation area, and for some chosen landslides with simpler morphological settings, to accumulation volume (see Figs. 3a and b).

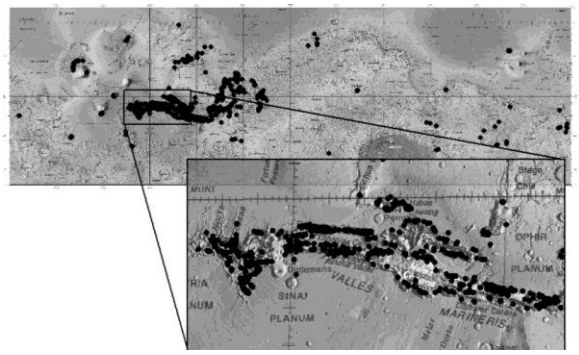

Figure 1 - Maps of the landslide inventory

We have also analysed the different landslide mobility in different areas (Fig.4), to verify the possible role of different controlling settings and/or environmental conditions at the time of the andslide occurrence. This is done by taking into account also the presence of morfological constrains.

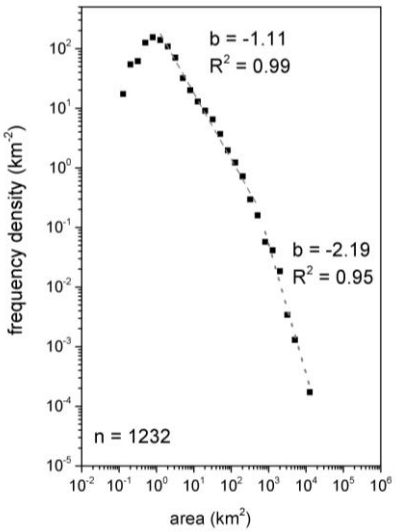

Figure 2 - Frequency distribution of mapped landslide areas with best fitting power law fuction parameters

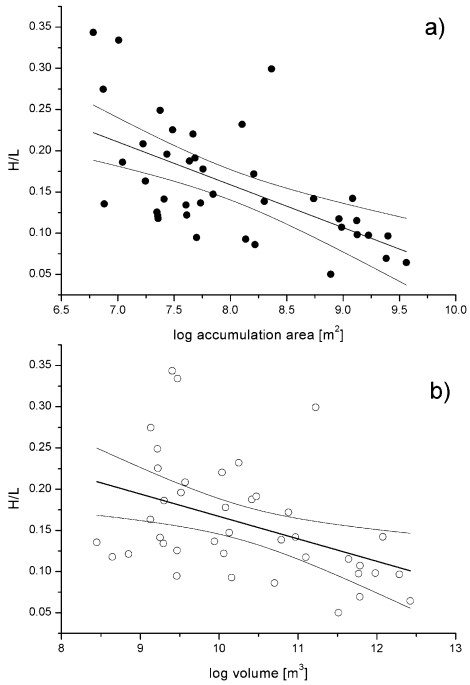

Figure 3 - H/L vs a) area and b) volume of 40 landslides

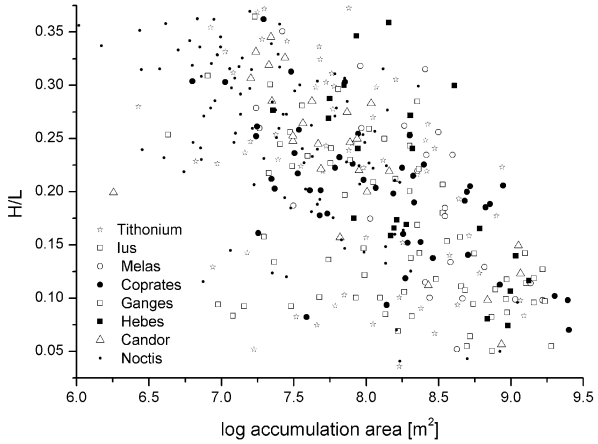

Figure 4 - H/L vs area plot for the present dataset subdivided for different sectors.

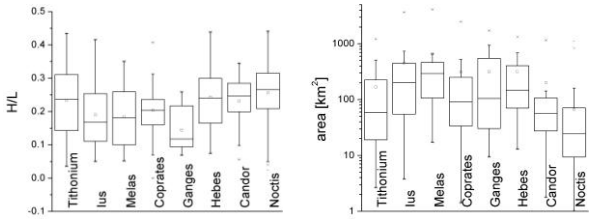

Figure 5 - H/L and area box plots subdivided for different sectors.

Conclusions: The dataset is still under construction and analysis are under completion. Nevertheless, the dataset, much wider than those presently available, confirm some of the previous observations concerning the mobility of martian landslides with respect to their Earth equivalent. At the same time this large dataset will allow to examine further in detail the controls by different morphogical, geological and environmental factors. The dataset will be made available after its completion.

References: [1] Shaller (1991) *Ph.D. thesis, Calif. Inst. of Technol.*. [2] Lucchitta, B.K. *JGR*, 84, 8097–8113 [3] Quantin, C., P. Allemand, and C. Delacourt (2004), *Planet. Space Sci.*, 52, 1011–1022. [4] Quantin, C., Allemand, P., Mangold, N., Delacourt, C. (2004). *Icarus*, 172, 555–572 [5] Brunetti, M.; Cardinali, M.; Fiorucci, F.; Guzzetti, F.; Santangelo, M.; Mancinelli, P.; Komatsu, G.; Goto, K.; Saito, H. (2011) *AGU, abstract #EP43A* [6]°Lucas, A., and A. Mangeney (2007), *Geophys. Res. Lett.*, 34, L10201, doi:10.1029/2007GL029835. [7]°Schultz, R.A., 2002. *Geophys. Res. Lett.* 29 (19). [8]° Soukhovitskaya, V., Manga, M. (2006), *Icarus* 180, 348–352. [9] Stark, C.P., Hovius, N. (2001)., *Geophys. Res. Lett.*, 28, 1091-1094